ICES Journal of Marine Science: Journal du Conseil
September 2008; Volume 65 (6) : Pages 982-994
http://dx.doi.org/10.1093/icesjms/fsn052

Proposals for the collection of multifrequency acoustic data

Rolf J. Korneliussen[1, *], Noel Diner[2], Egil Ona[1], Laurent Berger[2] and Paul G. Fernandes[3]

[1] Institute of Marine Research, PO Box 1870 Nordnes, 5817 Bergen, Norway
[2] IFREMER, BP 70 29280, Plouzane, France
[3] Fisheries Research Services, Marine Laboratory Aberdeen, PO Box 101, Victoria Road, Aberdeen AB11 9DB, UK

*: Corresponding author : R. J. Korneliussen: tel: +47 55 238500; fax: +47 55 238531; email address : rolf@imr.no

Abstract:

Acoustic surveys are used to estimate the abundance and distribution of many fish species, and have been based traditionally on data collected at a single acoustic frequency. Although it has been known for some time that the use of additional frequencies can provide information on the nature of the acoustic target, the knowledge and technology required to combine the so-called "multifrequency data" in an appropriate manner has been limited. The use of several transducers of different frequencies is now common on board research vessels and fishing vessels, so multifrequency data are often collected. In order for these data to be combined appropriately, their physical and spatial characteristics from each frequency should be as similar as possible. We detail the requirements deemed necessary to collect multifrequency data in an appropriate manner. They can be stringent and may not always be achievable, so we also consider the consequences of combining acoustic data originating in transducers with varying degrees of spatial separation and with different beam widths.

Keywords: data collection, multifrequency acoustics, species identification

Introduction

Acoustic surveys are used extensively throughout the world to determine the abundance and distribution of various types of marine and freshwater fauna and flora (Simmonds and MacLennan, 2005). Abundance is derived from density measurements that are the result of echo integration (MacLennan 1990) from a single acoustic operating frequency. Although data from more than one frequency were used by Cushing and Richardson (1955) to infer differences in scattering by frequency from different fish species, it was only in the 1970s that multifrequency data were used in earnest to identify scattering from various zooplankton size groups (Holliday, 1977; Greenlaw, 1979). This last work formed the basis of much of the effort to quantify and identify zooplankton in the 1980s (Greenlaw and Johnson 1983; Pieper and Holliday 1990), and coincided with concerted efforts to understand the theoretical basis for scattering by such groups, with the development of scattering models (e.g. Stanton 1989). These in turn led to practical techniques allowing for the discrimination of larger taxa in acoustic-survey data, such as krill (Madureira *et al.*, 1993) and, more recently, fish (Kang *et al.*, 2002; Korneliussen and Ona, 2002, 2003). Multifrequency acoustic data, therefore, have the advantage of providing information on the nature of the [acoustic] target of interest such that some discrimination by acoustic means may be possible (see Horne, 2000, for a review).

In most cases, acoustic-survey data are collected in a manner that is optimized for a single frequency, and less consideration is given to combining acoustic data from multiple frequencies. Although data manipulation and processing can allow data from many single frequencies to be combined, e.g. compensating for different transducers spaced apart along the ship by shifting the spatial reference of pings from one frequency to be aligned with the pings from another, optimal multifrequency data cannot be achieved from a system if the input data are not collected properly. Here, we propose methods for the collection of multifrequency acoustic data in a manner that is most appropriate for subsequent analysis.

Multifrequency data may be collected in various ways on board research and fishing vessels. They may be collected as if they were single-frequency data, i.e. with no intention of combining the different frequencies, or they may be collected with the explicit intention of combining all frequencies. Here, a common term for both these types of raw data is multiple single-frequency data. For these data to be analysed appropriately, the physical and spatial characteristics of acoustic data should be as similar as possible. Although direct comparability of data at different frequencies is impossible in all respects, ideally data should be as well suited as possible to allow for a combination of frequencies at a high spatial and/or temporal resolution. Acoustic data from several single frequencies are defined as ideal in this context if they can be used to generate combined frequency data at the same resolution as any one of the original single frequencies. The term "combined frequency data" refers to new artificial data generated from several of the original single-acoustic frequencies. This requires comparable physical measurements, carried out simultaneously from identical sampled volumes, limited only by the effective range of the highest frequencies.

It is desirable to keep the spatial resolution of acoustic data as high as possible in order to resolve scatterers, but it is also desirable to reduce acoustic variability to categorize the acoustic returns precisely. These two requirements are contradictory, because the averaging used to reduce the variability inherently also reduces the spatial resolution. Acoustic scattering has a stochastic nature, so there is a need to average (e.g. via smoothing) many acoustic measurements. **S**moothing inherently reduces the spatial resolution of the acoustic measurements. Some of the natural stochastic variation is reduced by the use of echosounders capable of rapid pinging and rapid sampling, by averaging samples from the same small elementary volume, but still there may be some stochastic variations attributable to radiation patterns, tilting, and the distribution of the scatterers in the measurement volume. As it is not clear how much averaging is needed to remove the stochastic variation of the measurements, it is reasonable, initially at least, to collect combined- frequency acoustic data at as high a resolution as possible.

Several recommendations are made and examined here under two major headings specifying the requirements of making data comparable: (i) physically, and (ii) spatially. Each proposal is numbered sequentially across these two headings, and these are finally summarized as a prioritized set. In practice, several of these proposals may not be achievable using current systems. When working with

hull-mounted transducers on research or fishing vessels, it is particularly difficult to obtain spatially comparable data. Different transducers are often mounted separately on the hull and may be several metres apart, so that the ideal case of co-locating all transducers at the same point is far from being fulfilled. Transducer size, beam width, and selectable pulse duration are generally optimized for target detection at each frequency, rather than for a combined analysis. Following the proposals, we examine the errors in echogram processing when data are collected from transducers spaced apart, or from transducers with different beam widths. Data from such equipment are termed "compromised" multifrequency data.

Many of the example settings are given with reference to Simrad echosounders and acoustic transducers, because these are currently the most commonly used instruments in marine fisheries acoustics. However, these are by no means the only instruments available, and operators wishing to develop along the lines we propose should approach manufacturers of their particular devices to obtain analogous settings where appropriate.

Requirements to make data physically comparable

Measurements of acoustic scatter at one frequency from fish or plankton should be comparable between equipment made by any manufacturer, provided the measurements are also spatially comparable. Physical measuresments refer to echosounder outputs such as s_v, s_A, target strength (TS) (and similar), and measurements that are used to calculate these, e.g. signal voltage, absorption, and sound speed. Absorption and sound speed are both components of range-dependent amplification used to calculate s_v, s_A, and TS. Absorption affects the physical measurements, whereas sound speed affects mainly spatial comparability, because it is seldom so wrong that it leads to significantly erroneous values of s_v, s_A, and TS. The range-dependent amplification is, therefore, treated under both the first and the final requirement .

Echosounder systems should be operated such that the linear-wave equations apply

Most theory within fisheries acoustics is based on linear-wave equations, which is typified by the use of range compensation in fisheries acoustics, commonly known as time-varied gain (TVG) (MacLennan, 1990; Simmonds and MacLennan, 2005). However, although non-linear acoustic interactions are always present, they are much reduced compared with linear sound, particularly when the acoustic power output from the transducers is reduced. These non-linear interactions take place in the insonified water-column and depend on the acoustic intensity and the acoustic frequency (Pedersen, 2006; Tichy *et al*., 2003). In order to reduce the effect of non-linear interactions, the power output from a transducer should be selected at a level where the non-linearly generated sound is negligible compared with linearly generated sound. In order to achieve this in, for example, the case of an echosounder using a Simrad ES38D transducer (38 kHz in Table 1), 15 kW m^{-2} or less output power is sufficient: for 60% transducer efficiency, this gives 25 kW m^{-2} or less input power, which is obtained by setting the maximum input power on the echosounder to 2500 W. Maximum input power settings for other Simrad transducers are given in Table 1. Note that the higher the frequency, the lower the input power needs to be to avoid generation of non-linear effects.

In the examples given in Table 1, most transducers weight the power across the transducer face to reduce side-lobe levels, i.e. to ensure that the power enforced on the outer elements is less than that at the central elements. The use of too high a power level for the transmission of sound leads to significant generation of sound at higher frequencies, through the non-linear effects. This will appear in the transmitted sound at the original frequency as loss in the signal in addition to the losses expected from absorption and geometric loss. Some of this loss is compensated for during the calibration process (Pedersen, 2006), but generally it is advisable to reduce the power to levels indicated in Table 1.

All echosounder and transducer systems must be calibrated

Foote (1982, 1989) and Foote *et al.,* (1987) described the generally accepted method of calibrating echosounders. The total error in the calibration method should be no more than 4%, i.e. the uncertainty in the measurements of s_A (nautical-area-scattering coefficient) attributable to calibration is approximately 4% (see Table 7 of Foote *et al.*, 1987, or Havforskningsinstituttet, 1994). The

components of the calibration errors are the equivalent beam angle ($\Delta\Psi$, 1.6%), time-varied gain (ΔTVG, 1.1%), target range (ΔR, 2.1%), and target accuracy (ΔTS, 2.2%), i.e. the accuracy of the calibration sphere. The error-components are squared and summed to give the 4% combined error: $\Delta\text{Cal} = [(\Delta\Psi)^2 + (\Delta\text{TVG})^2 + (\Delta\text{R})^2 + (\Delta\text{TS})^2]^{0.5} \approx 4$. Foote *et al.* (1987) claim that it is realistic to reduce calibration error to ~3% at 38 kHz by taking oceanographic measurements at the time of calibration to improve the estimate of the target range, i.e. reducing ΔTVG and ΔR. During calibration exercises in the sheltered fjords of Norway, it is realistic to achieve a total uncertainty of the calibration close to 3–4%: this may not be the case in many other places. At a workshop on hydroacoustic instrumentation (ICES, 1994), it was noted that a change in level of 0.5 dB (6%) between two calibrations should prompt some form of action. Ideally, two calibrations should take place for each major survey, one at the start and one at the end, allowing the system to be checked to ensure that it operated consistently throughout the survey.

The echosounder and transducers are often used in seawater far from the location of the calibration. Moreover, calibration of an echosounder system is in principle valid only when the transducer is used at the same depth as during the calibration exercise itself: this condition is largely met for transducers on fixed platforms. An echosounder connected to a transducer used at varying depths, e.g. a transducer mounted on a drop-rig or on a towed vehicle, should take the transducer depth into consideration when the backscatter is calculated. Protruding instrument-keel-mounted transducers (Ona and Traynor, 1990) should also be calibrated with the keel extended to the depth where it is most likely to be used. Transducers mounted on some other platform such as a drop-frame or a towed vehicle should be pressure-stabilized, but they still need to be calibrated at several depths. Note that the pulse-transmission delay (see below) should be accounted for, to obtain both the correct distance to the calibration sphere and the correct TVG start-time delay (see Fernandes and Simmonds, 1996). Irrespective of this, the calibration spheres should be as large as possible to increase their TS and weight, to reduce motion and interference from fish, and be deployed at a range as far as practically possible from the transducer.

In the case of the Simrad EK500 echosounder, all ranges are calculated relative to the transmitter trigger pulse inside the electronic circuits, i.e. the depths are not corrected for the total-system delays neither in the echogram (mean volume backscattering strength) nor the TS data (pers. comm. with Haakon Solli, Simrad). The recorded MVBS ranges should, therefore, be corrected with a total-system delay (see below). The depth at which the TS measurement is made is more difficult to correct because the first signal detected defines the depth.

The TVG was originally calculated from the depth of the front of the pulse, and did not consider the total-system delay. The TVG-delay compensated for in version 5.30 of the standard operating software in the EK500, is three times the sample interval plus half the pulse duration. In practice, this means that the TVG will be correct if a standard version of the EK500 is used with a "wide" bandwidth, because of the 3 × sample interval, but wrong otherwise. As an example, 38kHz/WIDE will estimate the total-system delay to be 3 × 10 = 30 cm, close to the measured 30 cm and calculated 29 cm. Special custom-made versions of programmable, read-only memory (PROM) available for the EK500 use 2-cm sample intervals and will, therefore, not compensate sufficiently. This is, however, a minor problem at large distances.

In the case of the new Simrad EK60, the centre of gravity is calculated for each pulse, so the start of the pulse should be a half-pulse duration before the centre of gravity. The TVG is calculated for each sample before it is eventually used in any calculations. The total-system delay is currently not accounted for in the EK60. This means that the range from the transducer to the volume-segment of measured backscatter is slightly too large, and the TVG applied to those measurements is slightly too large when volume backscatter, s_v, is calculated. The delay should be accounted for as described below for the correction of range to improve spatial overlap. At short ranges, s_v should also be corrected. Simrad says that the centre of gravity is used to calculate the range to single targets and that the total-system delay is not accounted for.

Noise should be insignificant

In general, noise is all the unwanted signals, including transmitted sound backscattered from wind-generated bubbles. It is, however, difficult to separate free bubbles from swimbladders in small fish or

bubbles generated for buoyancy by some types of plankton. A proper definition of noise is needed before developing a model to remove it. The definition of noise according to Korneliussen (2000) is "if the intended signal is defined as all transmitted sound backscattered onto the transducer surface, then noise is everything else." Sound generated by ships, animals, collapsing bubbles, wind, or sea are noise in this case, as is instrument noise not associated with the transmission of sound. Under this definition, backscattered sound caused by unwanted electrical signals in the transmit part of the echosounder is not noise, nor is sound backscattered from bubbles. When acoustic data are corrected for noise, and the noise is uncorrelated with the backscattered signal from the targets, the maximum range of the acoustic data is limited by the sampling volume of the beam (Ona, 1987; Foote, 1991). The acoustic-sampling volume is the volume where all targets of interest, at all orientations, are acoustically visible in all parts of the sampled volume for the ranges used: it is species- and density-dependent. Foote (1991) described the statistical properties of the sampling volume.

Measurements should not be biased by noise

To be able to quantify and remove noise, the noise and intended signal should not be correlated. Noise can be quantified and removed from the measured signal using the methods described by Korneliussen (2000), which requires the collection of passive acoustic data, or by Nunnallee (1987). These methods require that the echosounder does not truncate measurements below a threshold, and that noise is not removed automatically by an internal algorithm. In the case of the Simrad EK500 the "noise margin" should be set to 0 dB; fortunately, the new Simrad EK60 has no noise-removal feature to worry about.

In the absence of passive acoustic data, the data needed to quantify noise may be selected according to the scheme suggested by Korneliussen (2004). Although backscatter from bubbles is not noise according to the definition above, bubbles associated with the wash from the hull of a vessel are undoubtedly unwanted components of the backscatter within fisheries acoustics. It is, therefore, suggested that acoustic transducers be mounted on the bottom of a protruding instrument keel (Ona and Traynor, 1990), such that they can be lowered below the bubble layer to reduce unwanted backscatter from bubbles created from the wash of a ship's hull.

Noise should not reduce the acoustic sampling volume

This requirement is to ensure that noise does not influence the spatial comparability of the acoustic data. The TVG function compensates the acoustic measurements for range, and the calculations are based on a detection area A at range R. If noise exceeds the detection threshold, the area where the echosounder can detect targets is less than A, so the sampling volume is reduced. In general, the distance from the transducer at which data are considered valid should be reduced, rather than trying to correct data collected from a reduced sampling volume (see below). The data, therefore, should not be used beyond a range R at which noise starts significantly limiting the sampling volume of any target of interest (Ona, 1987; Foote, 1991).

The range R is where the sampling volume V starts being reduced, e.g. where volume backscatter s_v is no longer proportional to R^2. Strictly speaking, the measured data can be corrected if the reduction of the sampling volume between ranges R and $(R + \Delta R)$ is known. Note, however, that the range R where the sampling volume V starts being reduced obviously depends on the TS. Therefore, if a measured volume contains different species, and/or different sizes of each species, each of those would need their own correction function. The compromise is to use a common range, R, for all targets. In rare cases it may be possible to estimate functions at each frequency to correct for the reduction in the acoustic sampling volume. This would be the case for acoustic data collected where there was only one target of interest, of essentially one size, e.g. Norwegian spring-spawning herring 33 cm long in Ofotfjord during most winters between 1988 and 2006.

Interference between frequencies should be insignificant

If the echosounder system, i.e. the echosounder electronics, acoustic transducers, and connection cables, at any single frequency is interfered with by a system operating at another frequency, the signal and noise are correlated, such that the algorithms known to remove noise cannot be used. The interference can be checked but, ultimately, a solution must be provided by the echosounder manufacturers to avoid interference between frequencies, e.g. by offering appropriate selection of

acoustic frequency, bandwidth, and transducer input power. Further, the electronics used at one frequency should not interfere with the electronics used at another frequency, but this is usually not a problem. A narrow bandwidth in the system will reduce the problem of acoustic interference, but will exacerbate other problems related to the pulse envelope and total-system delay. Measurements to date indicate that interference between echosounder systems is a minor problem, at least in the measurements of backscatter. However, strong targets may be detectable at a frequency, e.g. 18 kHz, for a system running in passive mode if there is an active system running at a frequency close by, e.g., 38 kHz. Note also that in the case of moderate to strong non-linear generation of sound at frequency f_0, there will be unwanted sound-components that will interfere with systems at frequencies $2f_0$ and $3f_0$ (harmonics).

The choice of frequencies should, therefore, be sufficiently different so as to avoid mutual interference. Moreover, care must be taken to avoid choices which are harmonics of each other (e.g. 200 and 400 kHz), because of the non-linear generation of sound. When 200 and 400 kHz transducers were used together on board FRV "G. O. Sars" (IMR vessel 3), the second harmonic of 200 kHz (2 × 200 kHz = 400 kHz) generated so much sound, even with the input power recommended in Table 1, that the 400 kHz system could not be used. The latter is now being replaced with 333 kHz. Frequencies of odd multiples (3, 5, 7, …) should also be avoided because of the linear generation of sound. The frequency sequence (in kHz) 18; 38; 70; 120; 200; 333; 555; 926; 1543; 2572; 120 × 1.6667^n (n = 7, ...); is one of many possible options. This sequence gives a reasonable resolution for small targets, e.g. small zooplankton. The factor 1.6667 from 120 kHz is a convenient choice to select the next frequency, although there is nothing special about that number.

Requirements to make data spatially comparable

Figure 1 illustrates the problem associated with horizontal and vertical spatial overlap. Considering a cone as a simplified beam, two such beams of equal beam width θ irradiate two partly overlapping discs of equal size. At range R from the transducers, the fraction horizontal overlap (O_h) of two beams with beam width θ is:

$$O_h = \left(\frac{2\alpha}{\pi}\right) - \frac{a\sin(\alpha)}{R\pi\tan\left(\frac{\theta}{2}\right)}, \qquad (1)$$

where $\alpha = \cos^{-1}\left(\frac{d}{2R\tan\left(\frac{\theta}{2}\right)}\right)$, d is the separation distance between the transducer centres (m), θ the 3 dB beam width of the beams (rad), and R is the distance (range) from the transducer face (m).

Figure 2 shows O_h as a function of R for beams of width 7°. Note that O_h is not a measure of horizontal overlap between beams of different widths, because it is obviously meaningless to calculate mutual overlap for beams of different width. Only 56.6% of the backscatter measured within 11° is, on average, also within 7° of the same beam generated from a transducer radiating as a perfect circular piston, at all ranges. This is calculated from the two-way Bessel directivity functions of intensity multiplied by the ensonified area. For real beams, the level of the side lobes is less than the Bessel directivity, so 60% within 7° may be a better estimate for real beams than 56.6%.

The fraction-vertical overlap (O_v) for pulses of equal duration and shape between data collected at two acoustic frequencies, with similar beam width, is defined as

$$O_v \equiv [1 - \mathrm{abs}(\Delta v_1 - \Delta v_2) / \Delta z], \qquad (2)$$

where Δv_1 and Δv_2 are the vertical offset distances attributable to total-system delays, and Δz is the vertical resolution.

O_v is increased either if $(\Delta v_1 - \Delta v_2)$ is decreased or if the vertical resolution is decreased by increasing Δz. O_v can be improved if data are collected at a sufficiently high resolution provided the 3 dB beam widths are the same. Echosounder-pulse envelopes differ from an ideal square pulse, especially for narrow bandwidth and wider beams at low frequencies, e.g. 18 kHz. This makes the result of the vertical shifting of data at 18 kHz more uncertain. The correlation of vertically shifted data at 18 kHz relative to any of the other frequencies does not provide a significant improvement for sample data tested.

The fraction-spatial overlap (O_s) between the beams at different frequencies is defined as:

$$O_s \equiv O_v O_h \tag{3}$$

There is no strict requirement with respect to the overlap required for the generation of combined frequency echograms, but a $O_s \geq 0.85$ seems reasonable. In the case of the 38 and 120 kHz transducers on the FRV "G. O. Sars", as shown in Figure 3a (IMR vessel 2), where the transducers' centres are 39.5 cm apart, a O_s of 0.85 is achieved at 28 m. For the 38 and 200 kHz transducers spaced 67.5 cm apart, $O_s = 0.85$ at 47 m. For methods involving division or multiplication of data at two frequencies, $O_s = 0.85$ gives an uncertainty of about 15% in the result, in addition to the measurement uncertainty. O_s can never be better than O_h. The transducer configuration for the newer vessel, FRV "G. O. Sars" (Figure 3b; IMR vessel 3), was designed specifically to enhance spatial overlap of the beams, and shows a significant improvement on the configuration in the previous vessel: a**n** O_s of 0.85 as calculated by equations (1) and (3) is achieved 13–34 m below the transducers, depending on which beams are compared.

Further considerations of non-ideal situations, where data do not overlap because of either transducer spacing or different beam widths, are considered later.

Pulse lengths and pulse shapes should be identical at all frequencies

The nominal pulse lengths become equal when the pulse durations are equal at all frequencies. Equal nominal pulse durations at all frequencies are, therefore, a necessary requirement. The requirement of equal pulse shape also requires equal bandwidth in the system, which is more difficult to achieve.

A pulse duration of 1.0 ms is sufficient for the pulse envelope to stabilize in 18 kHz echosounder systems with common bandwidths. Such a pulse duration should, therefore, be used across all frequencies; shorter pulse durations would be sufficient if 18 kHz data are not used. Older equipment may require manufacturer modifications: in the case of the Simrad EK500, the same adaptation (PROM) that delivers 2-cm samples across all frequencies can be configured to deliver 1.0-ms pulse durations. If the special EK500 PROM is not available, a short pulse duration should be used for 12–27 kHz, medium for 38–70 kHz, and long for 120 kHz and above. In the case of the new Simrad EK60, it is possible to set the pulse duration to 1.0 ms for all frequencies. Wide bandwidth, 10% of centre frequency, is recommended for the Simrad EK500 for 70 kHz and below, and narrow bandwidth, 1% of centre frequency, for 120 kHz and above. The bandwidths for the EK60 are calculated by the system. When using 1-ms CW pulses, these are: 1.6 kHz at 18 kHz, 2.4 kHz at 38 kHz, 2.9 kHz at 70 kHz, 3.0 kHz at 120 kHz, 3.0 at 200 kHz, and 3.1 kHz at 364 kHz.

Individual pings should be identifiable in the data files at all times

This requirement ensures that simultaneous pings of different frequency can be identified and compared. It is insufficient to count pings in a datafile, because pings are occasionally lost, and the ping rate may be different when several echosounders are used simultaneously. Time should be registered when the echosounder is triggered to transmit, and should be stored with a resolution sufficiently high to avoid two pings at the same frequency being registered at the same time. A time resolution of 0.01 s is sufficient for such purposes; a resolution of 1.0 s is not.

Acoustic sampling volumes should be similar at all frequencies for comparable ranges to the scatterers

Targets of interest should be visible acoustically in all parts of the sampled volume for the ranges used (Foote, 1991). Provided there is insignificant noise, this implies similar half-power beam widths and

that all transducers should have the same centre, including identical transducer depth, and the same acoustic axis for the transducers.

This point is to achieve maximum horizontal overlap between the beams, but this is generally not possible. At best, transducers with similar beam widths should be mounted at the same depth and with the same acoustic-axis orientation. The smallest transducers should be placed in the middle in order to reduce the average distance between them. Standardizing the 3-dB beam widths to approximately 7° is a reasonable compromise between long range and wide beam width, to cover a large volume. For commercial low-frequency transducers, for example 18 kHz, generated beams of 11° may be the smallest achievable, and hence closest to 7°. The transducer faces should be adjusted to give the same orientation of the acoustic axis of all transducers if this cannot be done electronically: the acoustic axis is expected to be very close to a vertical straight line. Horizontal distance between the transducers will result in errors that are discussed further below. The effect of the horizontal offsets is reduced with increasing range from the transducers because of the conical shape of the beams. Therefore, the fraction-horizontal overlap (O_h) increases with depth.

Transmission of pulses should be simultaneous at all frequencies

In order to sample as similar a volume as possible, pulses from individual transducers (frequencies) should be transmitted at exactly the same time and incorporate appropriate system delays (to achieve maximum vertical overlap). For equal bandwidth in the systems, there will be no differences in the total-system delays (see above). However, in practice, the systems at different frequencies will have different bandwidths, and therefore, also different total-system delays, which have to be compensated for in some way. Total-system filtering causes vertical offsets. Increasing the difference in total-system delay increases the O_v, and a reduction in vertical resolution reduces it. If the data samples are collected with a sufficiently high vertical resolution and the vertical shift is known, the samples can simply be shifted vertically. If data are not collected with a sufficiently high resolution, the effect could be reduced somewhat by smoothing the data with weights shifted vertically.

Synchronization

Pulse transmission is properly synchronized within each Simrad EK500 echosounder, which can accommodate a maximum of three frequencies. When operating more than one EK500, the slowest of the utilized sounders, the EK500a, should trigger the fastest, the EK500b, or preferably they should be connected to an external trigger unit. In the latter case, it may be difficult to use the common bottom depth-dependent ping-rate.

Using an external time source as input to all EK500s will synchronize time, but if data are logged with time in all EK500s synchronized continuously, e.g. by GPS time, experience has shown some strange side effects, such as the wrong time or a time-jump on one of the echosounders. This effect is avoided by manually setting the time once to, say, GPS time, then switching back to the now corrected internal EK500 clock. Setting the EK500 to satellite time is done by setting the parameter "/UTILITY MENU/External Clock=Serial" to set the time, then "/UTILITY MENU/External Clock=Off".

In the Simrad EK60, which can incorporate up to seven transducers (frequencies) simultaneously, pulse transmission is properly synchronized for all transducers (frequencies).

System delays should be incorporated

Calculation of the delays from the echosounder's internal-trigger pulse are straightforward provided the electronic characteristics of components of the system are known. It is not recommended to compensate for the total-system delay until theoretical delays are verified by measurements.

Ona *et al.* (1996) measured the delays with a standard version of the Simrad EK500 software. Measurements and calculations were consistent, and showed that the total-system delay (in s) at frequency f (Hz) when non-composite[1] transducers were used were:

[1] The term "composite transducer" refers to the way the acoustic transducer is designed. The ceramic is cut into several thin rods, e.g. 2 mm × 2 mm cross-section, where the length of the rods defines the main acoustic-resonance frequency. Several rods are glued together in a regular pattern. By doing so, most of the unwanted resonance modes cannot be excited, while the main resonance can still be used. The removal of unwanted modes increases the frequencies where the transducer can be used. The use of glue between the rods also increases the

- Total-system delay for wide bandwidth (10% of the centre frequency): 14.8/f (s);
- Total-system delay for narrow bandwidth (1% of the centre frequency): 44.6/f (s).

The vertical shift for wide bandwidth is then close to 1480(14.8/f)/2 (m) for the EK500, which for 38 kHz is 29 cm. In the expression, 1480 m s^{-1} is the sound speed, and the division by 2 is to account for two-way transmission. Depths associated with the measurements of MVBS in the Simrad EK500 are not corrected in the echosounder-output data.

Similar calculations for the total-system delay have also been done for the Simrad EK60 (H. Nes, Kongsberg AS, pers. comm.), but calculations have not been as well verified as those for the EK500. The system delays attributable to the digital filters in the EK60 are zero. The theoretical total-system delay at the frequency f (Hz) for the Simrad EK60 consists of the delay of the hardware and of the transducer:

- System delay for Simrad EK60 hardware (GPT): 4.5/f (s);
- Delay attributable to non-composite transducer (Q-factor = 4): 2.5/f (s);
- Delay attributable to composite transducer (Q-factor = 2.5): 1.5/f (s)

Currently, the Simrad transducers at 70 kHz and above are composite. These give a vertical shift for EK60 close to 1480(7.0/f)/2 (m), which for 38 kHz is ~14 cm. Table 2 shows the vertical offsets attributable to system delays in the EK500 and the EK60 for common settings and transducers, as calculated from the formulae above at different frequencies relative to 38 kHz.

Correct sound speed and absorption coefficient should be applied

Sound speed and acoustic absorption can be calculated from the formulae of Francois and Garrison (1982a, b). Both the sound speed and the absorption change with changing salinity, temperature, and depth (pressure). When salinity, temperature, and depth are known, the formulae give an accurate value for sound speed. Therefore, it would be necessary to calculate new values continuously for sound speed and absorption to obtain the correct acoustic measurements. This in turn raises the possibility of erroneously inserting inappropriate values of sound speed and absorption into the echosounder.

The suggested solution is as follows: a conductivity–temperature–depth (CTD) probe needs to be employed in the survey area at the beginning of each survey to provide the required data. It is probably sufficient to use the same sound-speed profile and the same frequency-dependent absorption throughout the whole survey, and probably also good enough to use the same sound speed throughout the water column. If a depth-specific sound speed is used, the CTD profile used to calculate the sound-speed profile should follow the acoustic data. The CTD profile used to calculate sound speed and absorption should, naturally, be taken in the survey area. It is, for example, poor practise to use the CTD profile taken at the calibration site to calculate sound speed and absorption in the survey area if the two areas are far apart or different oceanographically.

Compromised data – use of data that are not comparable in all respects

The ideal situation where two or more transducer axes overlap perfectly or have exactly the same beam width is virtually impossible to fulfil. What follows, therefore, is a discussion on studies conducted to estimate the error in multifrequency analyses when the data have been compromised with regard to beam overlap: specifically, studies were carried out for transducers installed on IFREMER's FRV "Thalassa" from 12 kHz to 200 kHz, with beam widths from 7° to 16° and distances between

transducer bandwidth, although as a positive side-effect of the transducer design. A non-composite transducer is composed of one or a few elements, where the length of the elements defines the main acoustic-resonance frequency. The cross-section of the elements could be, for example, circular with diameter 80 mm, which makes unwanted resonances more likely than with composite transducers.

transducer centres ranging from 0.4 m to 2 m. Transducers with axes spaced some distance apart and with different beam widths are likely to provide data with the most common compromised condition. In common with the new "G. O. Sars", the transducers of FRV "Thalassa" have been rearranged to have them as close as possible. All other requirements (identical pulse length and shape, simultaneous pulse transmission, etc.) are assumed to be fulfilled. Further, what follows concerns only echotraces obtained from large multiple targets such as fish schools, not single echoes.

If we define a O_s of 0.85 as a reasonable value for comparing data, this definition relies on the simple 3 dB definition of beam widths and does not cover all echoes contributing to the signal in the sample volume at a certain threshold. The proportion of the beam truly occupied by the school during the process of detection as it passes through the acoustic beam is not taken into account.

As the global process of school detection and generation of an echotrace is quite complex, instrument error was estimated approximately using simulations of echotraces of fish schools (see Diner, 2001). The simulations presented here rely on a simple backscattering model of fish, which has been manipulated according to an updated method described in Diner (2007). Simulations were conducted using several schools of different dimension and MVBS, at various depths, detected by three different commonly used nominal beam widths: 7°, 11° and 16°. The images obtained were processed with different thresholds. In these studies two main analyses can be performed on the school echotraces:

1. *Global MVBS.* In this case, the echogram from each frequency is processed separately and comparisons are made on whole echotraces at each frequency (i.e. average MVBS), extracted from each school. Based on simulations of two identical transducer directivities at different locations, the instrument error is estimated as the difference between the MVBS values calculated for the echotraces of the same school detected by two different beams of the same frequency.
2. *Ping-to-ping.* In this case, the data from two channels are combined on a ping-to-ping basis to generate a new synthetic or virtual echogram. Echotrace descriptors are then extracted from the virtual echograms. The instrument error is equivalent to the mean difference in VBSs from the school between the two beams at the same frequency.

Potential instrument errors are induced by the athwartship or alongship distance between transducers, and by differences in beam width. The errors do not affect all types of multifrequency analyses:

- the "global MVBS" is affected by the athwartship distance and the difference in beam width;
- the precision of the ping-to-ping analysis depends also on the alongship distance.

When considering the variation in school length and depth, and the various transducer positions and beam widths that are possible, a large number of permutations are possible, and they are quite complex to summarize. To illustrate the potential errors, the simulations were based on the detection of geometrically homogeneous ellipsoid schools through the directivity function of an acoustic beam. This complex process can be simplified by normalizing the results according to a realistic geometric hypothesis of the dependence of the error on the derived parameter N_{bi}, the dimension of the echotrace relative to the beam width (Figure 4):

$$N_{bi} = \frac{L_i}{2D_i \tan(B_i/2)} \quad , \tag{4}$$

where $B_i = 0.44 \times \theta \times (dST)^{0.45}$ as a valid approximation of the inverse Bessel function for directivity in the considered part of the beam, θ is the nominal transducer beam width (7° for example), dST is the difference between the MVBS of the school echotrace (S_{vi}) and the threshold, and L_i and D_i are the length and mean depth, respectively, of the school echotrace. Note that the beam width is estimated using the detection angle, B_i, not the nominal angle of the transducer (Diner, 2001).

Athwartship distance errors

In multifrequency analyses, the athwartship distance between transducers could have an effect on the results obtained because, for example, small schools could occupy the entire part of one beam and a smaller part of another (Figure 5). During the school-detection process with a single beam, the width of the schools detected is unknown. For convenience, therefore, it was assumed that school width and length were equivalent. The fact that only a part of the beam is occupied and that only the edge of the target is detected, causes cumulative attenuation effects resulting in, for instance, a drastic reduction in the MVBS of the school detected through this beam. The phenomenon is quite complex because the whole process of detecting the school must be considered, i.e. all successive school echoes from the start to the end of detection, in addition to considering that the school is not on the beam's central axis.

Simulations were carried out for four athwartship separation distances: 0.40, 0.70 m, 1.0 m, and 2.0 m. For an athwartship transducer distance of 0.40 m, instrument errors for MVBS remain low, mostly <0.25 dB regardless of *dST*, school depth, or relative size of the school. Therefore, this is a good value to aim for when installing transducers. Differences in MVBS from the simulations with different athwartship offsets allowed for the definition of empirical minimum N_{bi} values under the hypothesis that they are related to a given acceptable error in MVBS (E), school depth D_i, and *dST* factor. For an athwartship distance e_n (n in m):

$$e_{0.70}:\ N_{bi} \geq \frac{20}{D_i} + \frac{8}{E^{0.05}} - 0.03dST - 6.8 \quad ,$$

$$e_{1.0}:\ N_{bi} \geq \frac{20}{D_i} + \frac{8}{E^{0.05}} - 0.03dST - 6.6 \quad ,$$

$$e_{2.0}:\ N_{bi} \geq \frac{20}{D_i^{0.8}} + \frac{8}{E^{0.05}} - 0.05dST - 6.3 \quad .$$

These relations are approximations of the influence of depth of the school and the threshold, and allow for rapid selection of schools, which can be processed with a potential instrument error that does not disrupt further multifrequency analyses. Figure 6 gives a general representation of these limit N_{bi} values. At shallow depths, e.g. 15 m, with a *dST* of 10 dB, the N_{bi} limits are high, especially for large athwartship distances. Generally, the N_{bi} limit decreases when *dST* increases, i. e. when the processing threshold decreases.

Alongship distance errors

When transducers are spaced apart longitudinally by several metres, instrument errors are induced at the start of detection, because one beam detects a school some pings before another and, conversely, loses the school before the other, at the end of detection (Figure 7). If the transducers are not too far apart (<6 m, for example), the echotraces of the same school, detected by the two beams are, in most cases, similar, and the global MVBS is not subject to a large instrument error. This is not the case for ping-to-ping analysis. During the phases of the start or end of school detection, there is a regular variation of the level of the received signal from one ping to another. This signal level, related to the proportion of the beam width occupied by the fish, increases until the beam is fully occupied. It then remains constant for some pings, the centre of the school or school kernel, and finally decreases as the proportion of the occupied beam lowers, until the end of school detection (Figure 8). If a comparison between frequencies is made, e.g. $MVBS_{F1} - MVBS_{F2}$, which is equivalent to the ratio of echo intensities I_{F1}/I_{F2}, the ratio would be high towards the end of detecting the school because I_{F2} is lower than I_{F1}, and vice versa at the start of detection.

In order to determine the extent of this phenomenon, different school sizes, depths, and MVBS were simulated. Errors attributable to alongship separation distances of 0.5, 1.0, 1.5 and 2.0 m were calculated (with a ping interval of 0.5 m). For an alongship separation distance of 0.5 m and a *dST* value of 5 dB, the instrument errors were <0.5 dB whatever the school size or depth. For an alongship separation distance of 2.0 m and a *dST* of 5 dB, the school depth must be >25 m in order to reduce the

instrument error to an acceptable level. With a *dST* of 10 dB or more, the errors remain high whatever the school size or depth.

One solution to this problem is to compensate for this alongship distance in term of ping numbers, i.e. to shift the frequency analysis by a number of pings equivalent to the distance. However, when vessel speed is fast (e.g. 10 knots) and ping rate low (1 ping s^{-1}), the distance between pings can be greater than the transducer alongship distance (~5 m in the example cited). Therefore, such a ping shift is unable to compensate for the separation distance. High ping rates and/or reduced vessel speed would give better results.

Errors of beam width

The underestimation of a school's MVBS is related to different parameters, but critically to the relative school and beam-width dimensions (Diner, 2001). Using different beam widths leads to the underestimation of various parameters, resulting in errors in the multifrequency analysis in the global MVBS approach. Shifted detection as a consequence of different beam widths generates problems analogous to the alongship separation of transducers in the case of a ping-to-ping analysis. In order to investigate this problem, simulations of school detection were carried out at different depths using four different beam widths: 7°, 8°, 11°, and 16°. In each case, the difference between the echotrace MVBS was calculated for the same school detected using two beam angles, $\theta 1$ and $\theta 2$: $\Delta\text{MVBS}(\theta 1, \theta 2) = [\text{MVBS}_{\theta 1} - \text{MVBS}_{\theta 2}]$.

When a school is detected by a vertical beam, its MVBS is systematically underestimated. This underestimate increases as the horizontal dimensions of the school become smaller relative to the beam width (i.e. low N_{bi} values). When a school is detected by two frequencies with the same beam width, the two underestimates are similar and do not affect the result of the multifrequency analysis. In the case of two different beam widths, the difference in the MVBS underestimate for the two directivities must be determined: this difference will be equivalent to the instrument error in a multifrequency analysis (global MVBS).

An algorithm to determine a correction in school descriptors (Diner, 2001) was used to investigate this. The underestimate in school MVBS in relation to N_{bi} is given by

$$dSv = \frac{2.56}{N_{bi} - 1} \quad (5)$$

The difference in MVBS for two different beam widths is then

$$\Delta MVBS(\theta_1, \theta_2) = dSv_{\theta 1} - dSv_{\theta 2} = 2.56\left[1/(N_{bi\theta 1} - 1) - 1/(N_{bi\theta 2} - 1)\right] \quad (6)$$

By combining the results of simulation, relationships between $N_{bi7°}$ and other nominal beam widths, i.e. $N_{bi8°}$, $N_{bi11°}$, and $N_{bi16°}$ were determined. The difference in MVBS coefficient can then be expressed in relation to $N_{bi7°}$ by adjusting the coefficients of Equation (6) as follows:

$$\Delta MVBS(7,8) = 2.56\left[1/(N_{bi7°} - 1) - 1/(0.87N_{bi7°} - 0.87)\right],$$

$$\Delta MVBS(7,11) = 2.56\left[1/(N_{bi7°} - 1) - 1/(0.59N_{bi7°} - 0.57)\right],$$

$$\Delta MVBS(7,16) = 2.56\left[1/(N_{bi7°} - 1) - 1/(0.46N_{bi7°} - 0.41)\right].$$

The potential errors for a range of N_{bi} values are given in Figure 9. In general, there are small errors for 7°/8°, in most cases <0.5 dB. For 7°/11°, or worse 7°/16°, unless the schools are very large ($N_{bi7°} > 7$), large errors are obtained, hindering comparison of the data obtained with a 7° nominal beam width (e.g. 38, 120, or 200 kHz) and an 11° (18 kHz) or 16° (12 kHz) beam width.

A possible solution in such cases is to limit the analysis to data from the school kernel, the portion of the detected school when the beams of the two frequencies are fully occupied by fish. Some pings at the start and end of school detection should, therefore, be removed from the analysis. This number

(of pings) is calculated, taking into account the larger beam width, but using the real detection angle, B_i:

$$B_i = 0.44 \times \theta \times (dST)^{0.45} \quad (7)$$

The relevant distance at the start and end of school detection, L_{pg}, is then

$$L_{pg} = 2D_i \tan(B_i / 2) \quad (8)$$

If the vessel speed is V_s (in m s^{-1}) and the ping rate P_g (in s), the total number of pings to be removed is

$$n_{pg} = \frac{2D_i \tan(B_i / 2)}{V_s P_g} \quad (9)$$

Some examples of numerical applications are given below:

$\theta = 11°$, $dST = 20$ dB => $B_i = 18.6°$,
$D_i = 150$ m, $V_s = 5$ m s^{-1}, $P_g = 0.5$ s, $n_{pg} = 20$;

$\theta = 11°$, $dST = 20$ dB => $B_i = 18.6°$,
$D_i = 50$ m, $V_s = 2.5$ m s^{-1}, $P_g = 0.5$ s, $n_{pg} = 13$;

$\theta = 11°$, $dST = 10$ dB => $B_i = 13.6°$,
$D_i = 150$ m, $V_s = 5$ m s^{-1}, $P_g = 0.75$ s, $n_{pg} = 12$.

Discussion

Our motivation in writing this paper was to improve automatic acoustic species identification at high spatial resolution, and therefore, the analysis of echotraces from biological targets, particularly fish schools small in size. At this stage, more effort needs to be allocated to improving echosounder systems and transducer platforms where they are used for multifrequency observations. In order to limit the instrument error induced by having transducers at different locations, the number of candidate schools that can be subject to multifrequency analysis will be limited, and this limits the number of small schools that can be considered. The suggestions for transducer arrangement (below) are directed towards the design of new research vessels, or for the rearrangement of transducers on existing research vessels. Preliminary results of this paper were used when FRV "G. O. Sars" was designed (Figure 3b), when the transducers of FRV "Thalassa", FRV "Dr Fritjof Nansen", FRV "Scotia", and FRV "Johan Hjort" were rearranged, and when the commercial FV "Libas" was designed. Designers of towed vehicles have also benefited from some of the ideas in preliminary versions of this paper.

Care must be taken, however, with regard to the relative size of a school compared with the beam width, because for small schools the instrument errors based on athwartship offsets and different beam widths may be greater than any differences attributable to their natural frequency response. The minimum range for the methods described are limited by the requirement that $O_s > 0.85$, and the maximum range is limited by the effective range of the highest frequencies which are, typically, 150–200 m for a 200-kHz system aiming to detect weak targets from vessel-mounted transducers. Most of the water column over the continental shelf may, therefore, be investigated at full survey speed. However, deeper fish and weak targets such as zooplankton must be investigated either by a combination of lower frequencies, or from towed vehicles equipped with similar instrumentation. Calibration of multiple transducers over the pressure range then becomes a fresh challenge (Ona and Svellingen, 1999).

To conclude, in order to collect multifrequency data of as high quality as possible, the actions below are proposed in order of priority.

1) Select multiple frequencies that avoid harmonic interference. One possible selection of frequencies is 18, 38, 70, 120, 200, 333, 555, 926, 1543, and 2572 kHz;
2) Choose transducers with similar, if not identical, beam widths;
3) Mount all transducers as close together as possible, with the smallest transducers in the centre;
4) Synchronize the transmission from the different transducers;
5) Ensure that each ping of each frequency is time-stamped at a resolution of at least 0.01 s;
6) Select the transducer power output at levels which preclude significant losses from non-linear effects, e.g. 250 W for 120 kHz, 110 W for 200 kHz;
7) Operate all frequencies with the same pulse duration, ping rate, and digitized sample length;
8) Collect data at the lowest possible threshold, e.g. –120 dB or less;
9) Calibrate all frequencies at least once per survey, ideally twice (at the start and end);
10) Apply appropriate sound speed and absorption coefficients;
11) Remove noise where appropriate, e.g. at greater depths at higher frequencies.

Where data have been compromised through one of the above criteria not being met, one or more of the following steps may alleviate some of the problems:

- Use as low a noise threshold as possible when processing the raw data;
- Average data over multiple samples to obtain equivalent sampling volumes;
- Compensate for alongship separation of transducers by shifting pings equivalent to the separation distance;
- Compensate for transducers with different beam widths by limiting multifrequency analyses to the school kernel.

Acknowledgements

The work leading to this document was carried out with support from the European Commission's Fifth Framework Programme (SIMFAMI project; Grant No. Q5RS-2001-02054).

References

Cushing, D. H., and Richardson, I. D. 1955. A triple frequency echosounder. Fishery Investigations Series II, 10(1). 18 pp.

Diner, N. 2001. Correction on school geometry and density: approach based on acoustic-image simulation. Aquatic Living Resources, 14: 211–222.

Diner, N. 2007. Evaluating uncertainty in measurements of fish-shoal, aggregate-backscattering cross-section caused by small shoal size relative to beam width. Aquatic Living Resources, 20: 117–121.

Fernandes, P. G., and Simmonds, E. J. 1996. Practical approaches to account for receiver delay and the TVG start time in the calibration of the Simrad EK500. ICES Document CM 1996/B: 17. 8 pp.

Foote, K. G. 1982. Optimizing copper spheres for precision calibration of hydroacoustic equipment. Journal of the Acoustical Society of America, 71: 742–747.

Foote, K. G. 1989. Spheres for calibrating an eleven-frequency acoustic-measurement system. ICES Document CM 1989/B: 3.

Foote, K. G. 1991. Acoustic-sampling volume. Journal of the Acoustical Society of America, 90: 959–964.

Foote, K. G., Knudsen, H. P., Vestnes, G., MacLennan, D. N., and Simmonds, E. J. 1987. Calibration of acoustic instruments for fish-density estimation: a practical guide. ICES Cooperative Research Report, 144. 69 pp.

Francois, R. E., and Garrison, G. R. 1982a. Sound absorption based on ocean measurements. 1. Pure water and magnesium sulphate contributions. Journal of the Acoustical Society of America, 72: 896-907.

Francois, R. E., and Garrison, G. R. 1982b. Sound absorption based on ocean measurements. 2. Boric acid contribution and equation for total absorption. Journal of the Acoustical Society of America, 72: 1879–1890.

Greenlaw, C. F. 1979. Acoustic estimation of zooplankton populations. Limnology and Oceanography, 24: 226–242.

Greenlaw, C. F., and Johnson, R. K. 1983. Multiple-frequency acoustical estimation. Biological Oceanography, 2: 227–252.

Havforskningsinstituttet (Institute of Marine Research). 1994. Acoustic calibration compendium. IMR, Bergen, Norway. Including: Contributions from the Institute of Marine Research, Norway, by K. G. Foote., H. P. Knudsen, and G. Vestnes. Contributions from the Marine Laboratory, Scotland, by D. N. MacLennan, and E. J. Simmonds (Norwegian title, but the compendium contains a series of papers on the topic of calibration in English).

Holliday, D. V. 1977. Extracting bio-physical information from the acoustic signatures of marine organisms. *In* Oceanic Sound Scattering Prediction, pp. 619–624. Ed. by N. R. Andersen, and B. J. Zahuranec. Plenum Press, New York.

Horne, J. 2000. Acoustic approaches to remote species identification: a review. Fisheries Oceanography, 9: 356–371.

ICES. 1994. Report from the ICES workshop on hydroacoustic instrumentation. ICES Document CM 1994/B: 9. 9 pp.

Kang, M., Furusawa, M., and Miyashita, K. 2002. Effective and accurate use of difference in mean volume-backscattering strength to identify fish and plankton. ICES Journal of Marine Science, 59: 794–804.

Korneliussen, R. 2000. Measurement and removal of echo integration noise. ICES Journal of Marine Science, 57: 1204–1217.

Korneliussen, R. J. 2004. The Bergen Echo Integrator post-processing system, with focus on recent improvements. Fisheries Research, 68: 159–169.

Korneliussen, R. J., and Ona, E. 2002. An operational system for processing and visualizing multi-frequency acoustic data. ICES Journal of Marine Science, 59: 293–313.

Korneliussen, R. J., and Ona, E. 2003. Synthetic echograms generated from the relative frequency response. ICES Journal of Marine Science, 60: 636–640.

MacLennan, D. N. 1990. Acoustic measurement of fish abundance. Journal of the Acoustical Society of America, 87: 1–15.

Madureira, L. S. P., Everson, I., and Murphy, E. J. 1993. Interpretation of acoustic data at two frequencies to discriminate between Antarctic krill (*Euphausia superba* Dana) and other scatterers. Journal of Plankton Research, 15: 787–802.

Nunnallee, E. P. 1987. An alternative method of thresholding during echo integration data collection. Paper presented at the International Symposium on Fisheries Acoustics, 22–26 June 1987, Seattle, Washington. 12 pp.

Ona, E. 1987. The equivalent beam angle and its effective value when applying an integrator threshold". ICES Document CM 1987/B: 35.

Ona, E., and Svellingen, I. 1999. High-resolution target-strength measurements in deep water. Journal of the Acoustical Society of America, 105: 1049.

Ona, E., and Traynor, J. 1990. Hull-mounted, protruding transducer for improving echo integration in bad weather. ICES Document CM 1990/B: 31.

Ona, E., Zhao, X., Svellingen, I., and Foote, K. 1996. Some pitfalls of short-range standard- target calibration. ICES Document CM 1996/B: 36.

Pedersen, A. 2006. Effects of nonlinear sound propagation in fisheries research. PhD dissertation, University of Bergen, Norway. 308 pp.

Pieper, R. E., and Holliday, D. V. 1990. Quantitative zooplankton distributions from multifrequency acoustics. Journal of Plankton Research, 12: 433–441.

Simmonds, E. J., and MacLennan, D. N. 2005. Fisheries Acoustics: Theory and Practice, 2nd edn. Blackwell Publishing, Oxford. 456 pp.

Stanton, T. K. 1989. Simple approximate formulas for backscattering of sound by spherical and elongated objects. Journal of the Acoustical Society of America, 86: 1499–1510.

Tichy, F. E., Solli, H., and Klaveness, H. 2003. Non-linear effects in a 200-kHz sound beam and the consequences for target-strength measurement. ICES Journal of Marine Science, 60: 571–574.

Figure legends

Figure 1. Schematic diagram of some of the spatial problems for the generation of high-resolution, combined-frequency echograms from data at two arbitrary, not co-located transducers, Transducer 1 and Transducer 2. Partial overlap, or at best horizontal offset, is the normal situation. The effect of horizontal offset decreases with increasing depth, whereas the effect of vertical offset remains. Reduction of the vertical resolution may reduce the problem of vertical offset.

Figure 2. Fraction-horizontal overlap (O_h) of two beams with similar 3-dB beam widths plotted as function of depth range (R) below the transducer for several distances (d) between two transducer centres.

Figure 3. Example of placement of transducers on the instrument keels of two research vessels. (a) FRV "G. O. Sars" (IMR vessel 2) (top view). (b) FRV "G. O. Sars" (IMR vessel 3) (top view).

Figure 4. School lengths as a function of N_{bi} , i.e. the dimension of the echotrace relative to the beam width, for different school depths and a fixed difference between school MVBS and threshold (*dST*) value of 15 dB. Each curve shows N_{bi} at a fixed depth D_i.

Figure 5. Schematic showing detection of a school by two different transducers spaced athwartship by a distance *e*, in the vertical (left) and horizontal planes (right). On the right panel, circles labelled A indicate when the beam is on the border of the school, and the school is not detected, circles labelled B indicate cases where the centre of the beam is on the border of the school where the beam is partially occupied by the school, and circles labelled C indicate cases where the school occupies the whole beam

Figure 6. N_{bi} limit values, i.e. the dimension of the echotrace relative to the beam-width limit values, as a function of school depth, calculated by empirical relationsships, for an error of 0.5 dB, difference between school MVBS and threshold (*dST*) of 20 dB (continuous lines) or 10 dB (dotted lines), and athwartship distances *e* of 0.7 m (red lines with diamonds), 1.0 m (blue lines with squares), or 2.0 m (green lines with circles.

Figure 7. Detection of a school by two beams, F1 and F2, spaced a distance apart alongship, in five successive transmissions.

Figure 8. Successive ping amplitudes for the mean depth of a 20-m-long simulated school (dotted line) located 25 m deep (simulated signal level in mV). Solid lines indicate the ratio of the signal level as detected by transducers separated by alongship distances of 0.5 m (green), 1.0 m (blue), and 2.0 m (red).

Figure 9. Potential errors, in relation to $N_{bi,7°}$, i.e. the dimension of the echotrace relative to the beam width, induced by using different nominal beam widths: θ = 8°, 11°, and 16°, compared with 7°.

Running headings

R. J. Korneliussen et al.

Proposals for the collection of multifrequency acoustic data

Table 1. Parameters and recommended maximum input power for common sizes of Simrad transducer.

Parameter	**Maximum input power per frequency (kHz)**							
	18	**38**	**70**	**70**	**120**	**200**	**333**	**400**
Approximate transducer area (10^{-3} m^2)	200	100	30	12	10	4.4	1.6 *	1.1
Approximate 3-dB beam width (°)	11	7	7	11	7	7	7	7
Recommended maximum input power for 60% electro-acoustic efficiency (W)	5000	2500	750	300	250	110	40	28

* Transducer area estimated by authors.

Table 2. Difference in vertical offset in EK500 and EK60 for common settings and transducers at different frequencies relative to 38 kHz. Δ18 is the difference between offsets at 18 kHz and 38 kHz.

Echosounder	**Δ18 (cm)**	**Δ38 (cm)**	**Δ70 (cm)**	**Δ120 (cm)**	**Δ200 (cm)**	**Δ333 (cm)**
EK500	32*	0*		–0.5†	–12.0†	
EK60	15	0	–7‡	–10‡	–11‡	–12‡

* EK500 “WIDE” filter

† EK500 “NARROW” filter
‡ Composite transducer

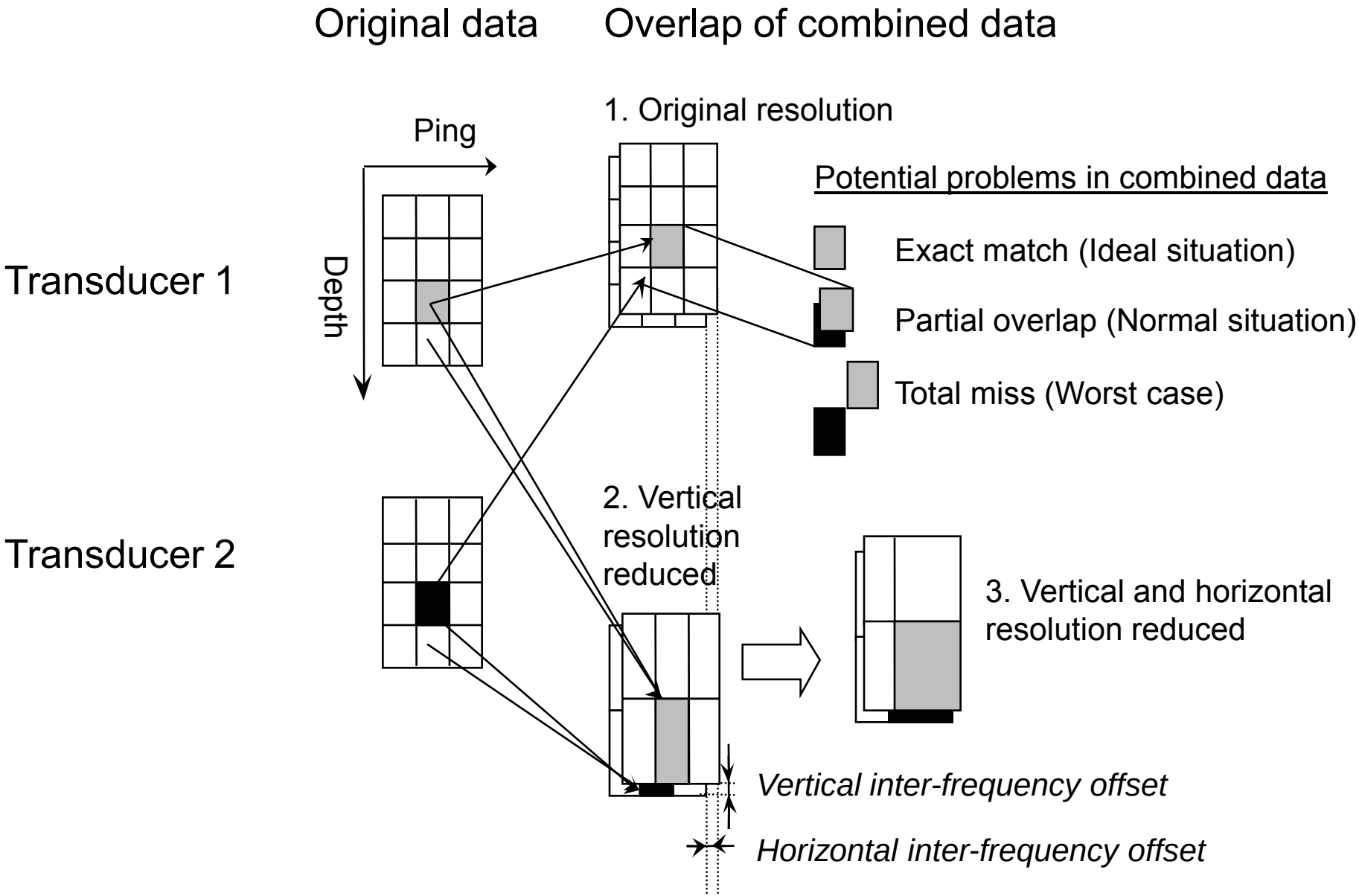
Original data
Overlap of combined data
Transducer 1
Transducer 2
Ping
Depth
1. Original resolution
Potential problems in combined data
Exact match (Ideal situation)
Partial overlap (Normal situation)
Total miss (Worst case)
2. Vertical resolution reduced
3. Vertical and horizontal resolution reduced
Vertical inter-frequency offset
Horizontal inter-frequency offset

Fig.1

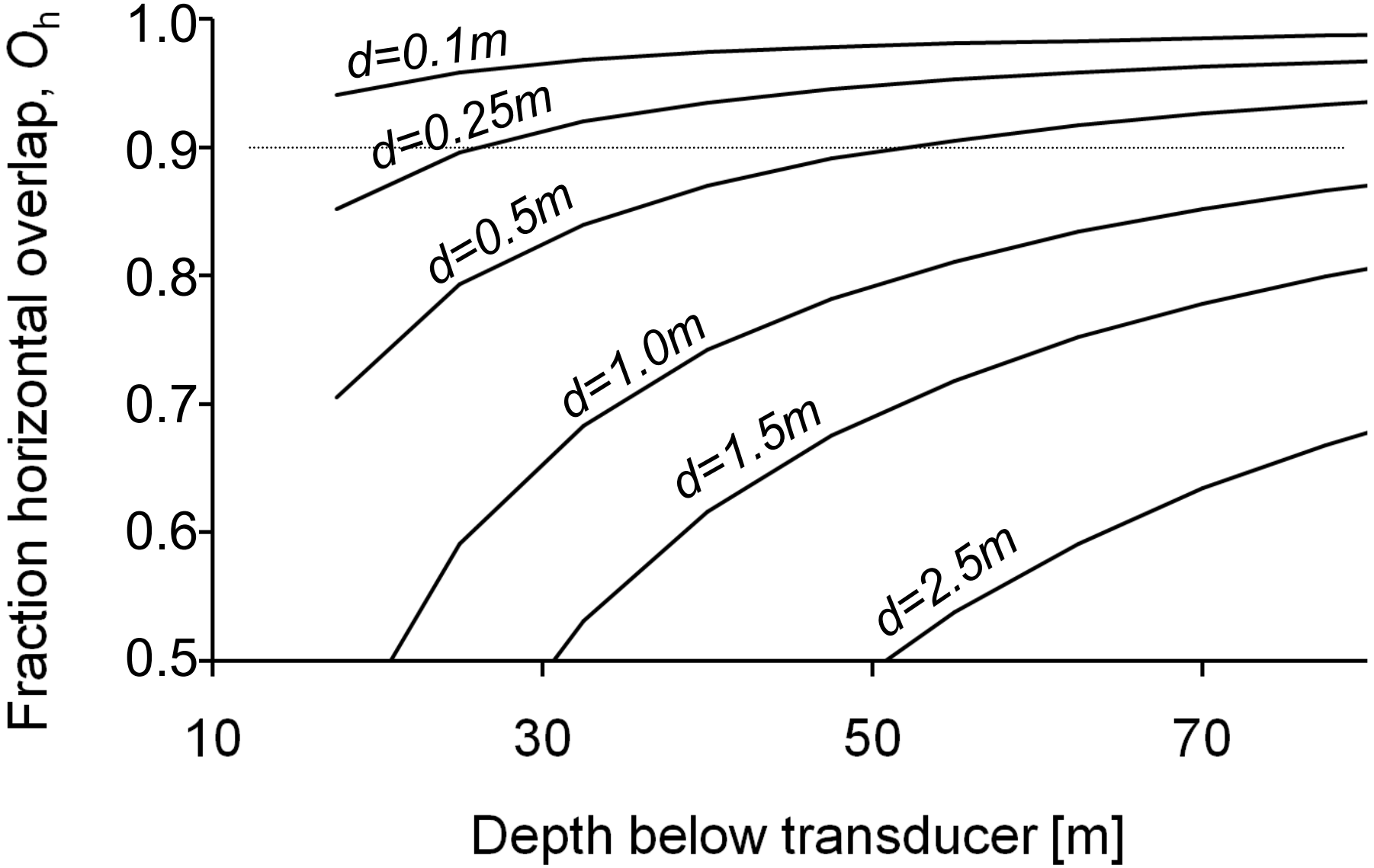
Fraction horizontal overlap, O_h
1.0
0.9
0.8
0.7
0.6
0.5
d=0.1m
d=0.25m
d=0.5m
d=1.0m
d=1.5m
d=2.5m
10
30
50
70
Depth below transducer [m]

Fig.2

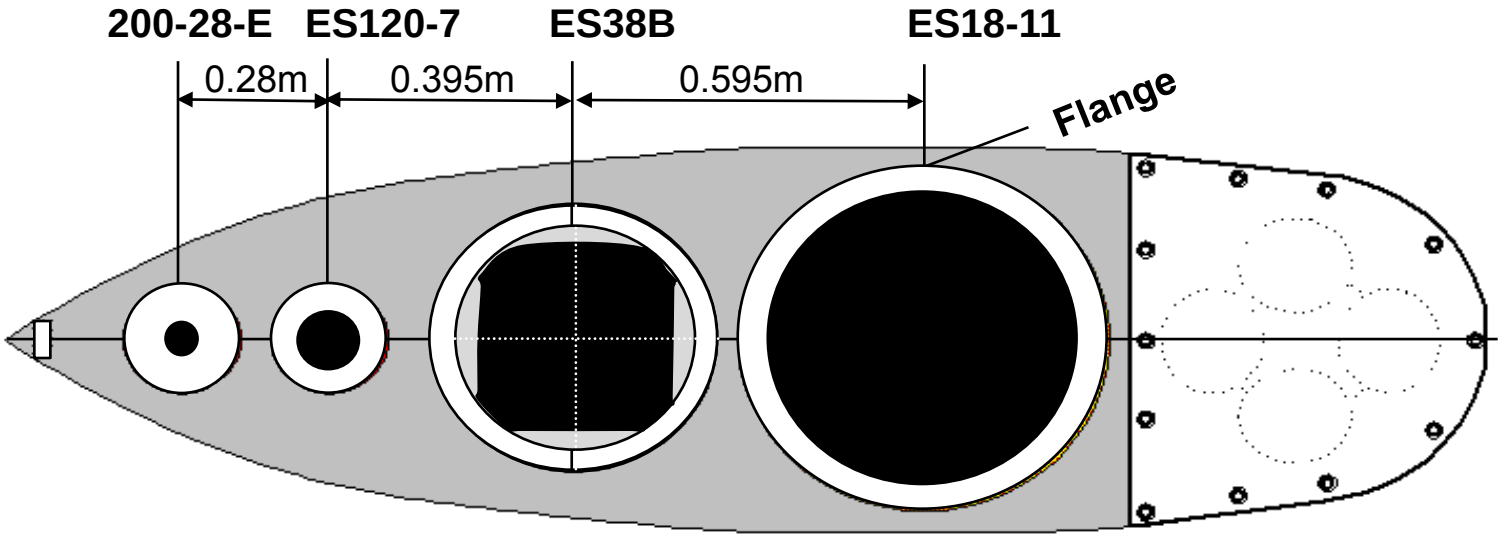

a) Transducer mounting on protruding keel on RV “G. O. Sars” (IMR vessel 2) (top view)

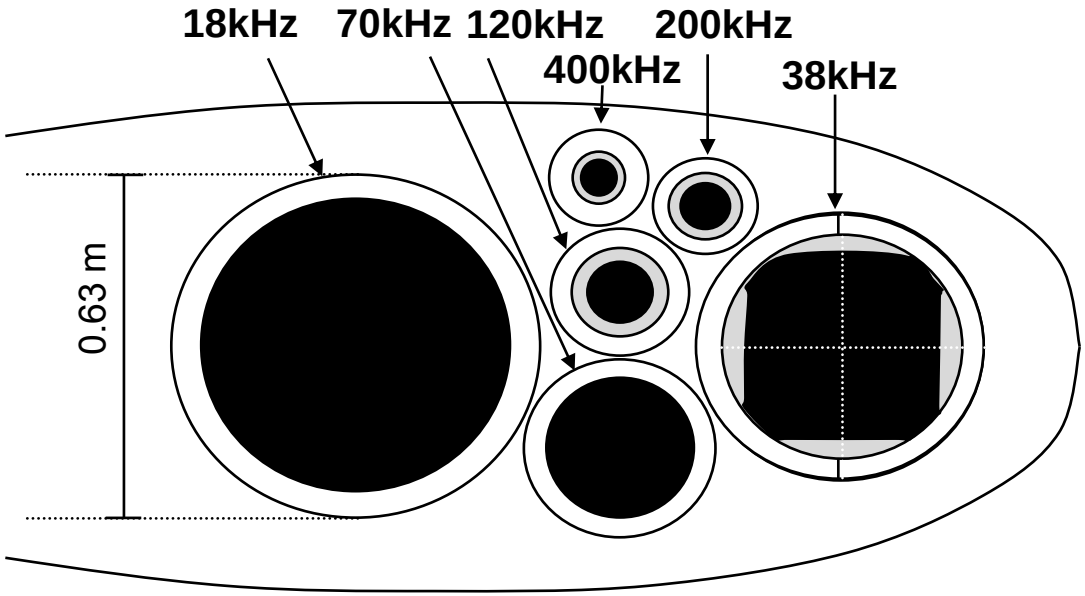

b) Transducer mounting on protruding keel of RV “G.O. Sars” (IMR vessel 3) (top view)

Fig.3

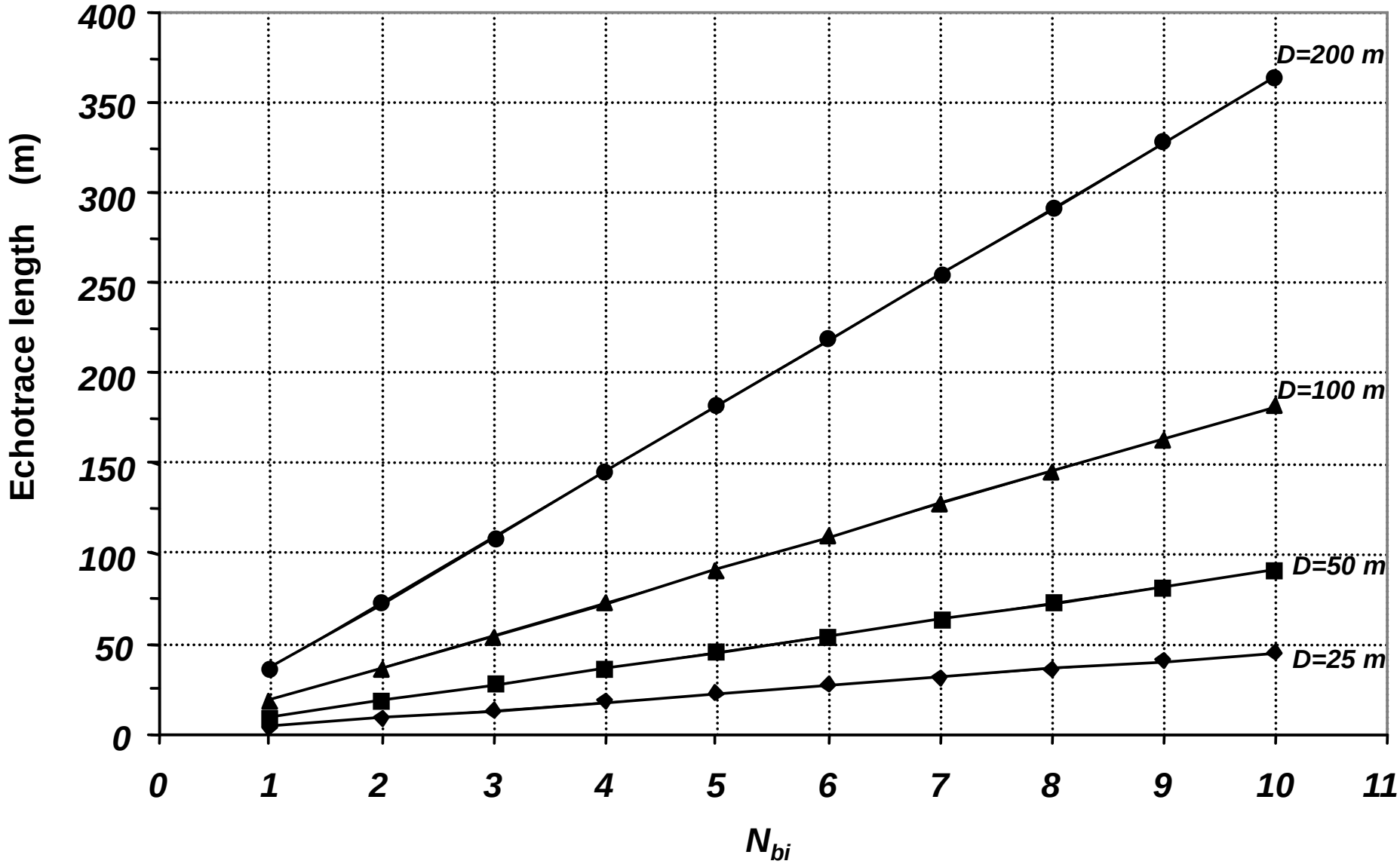
Echotrace length (m)
400
350
300
250
200
150
100
50
0
0
1
2
3
4
5
6
7
8
9
10
11
N_{bi}
D=200 m
D=100 m
D=50 m
D=25 m

Fig. 4

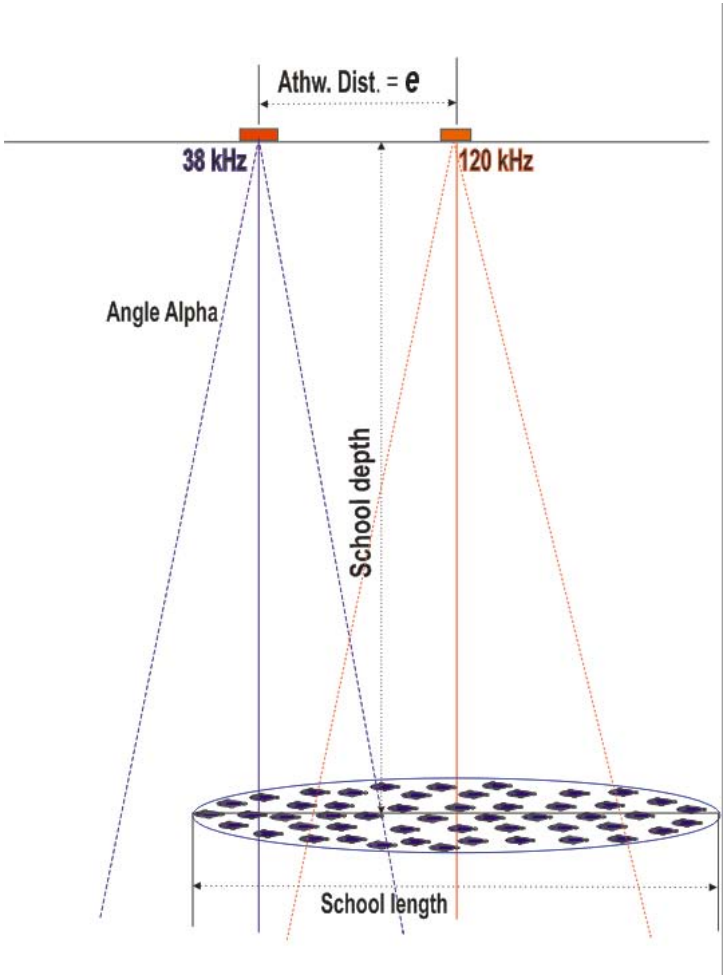
Athw. Dist. = e
38 kHz
120 kHz
Angle Alpha
School depth
School length

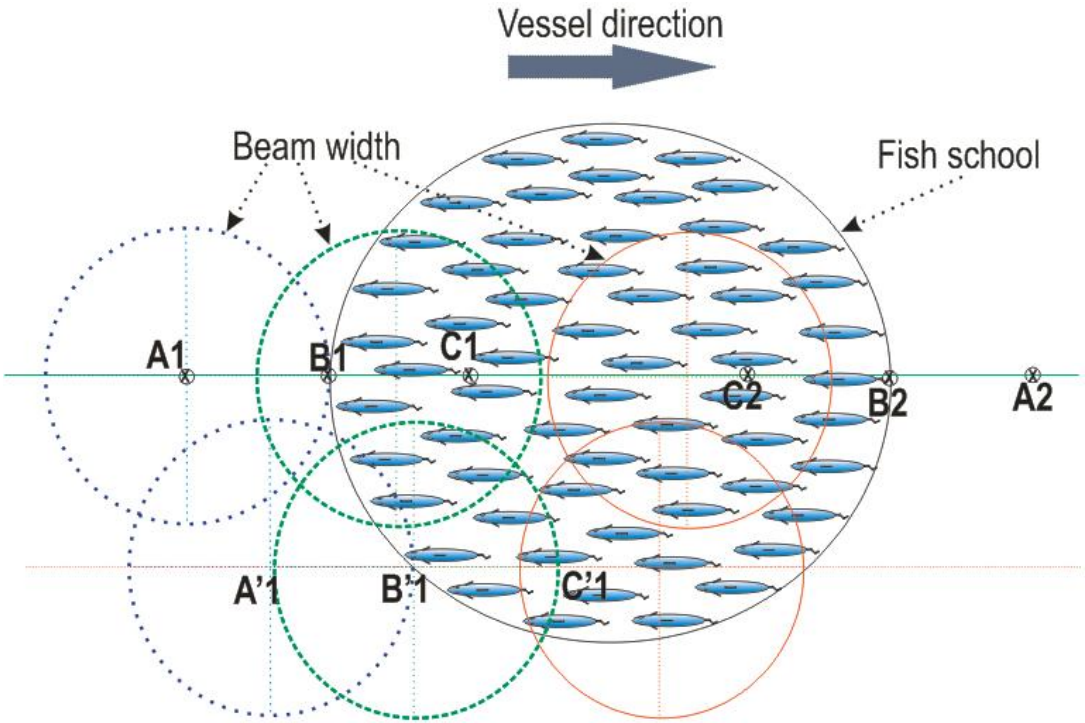
Vessel direction
Beam width
Fish school
A1
B1
C1
C2
B2
A2
A'1
B'1
C'1

Fig. 5

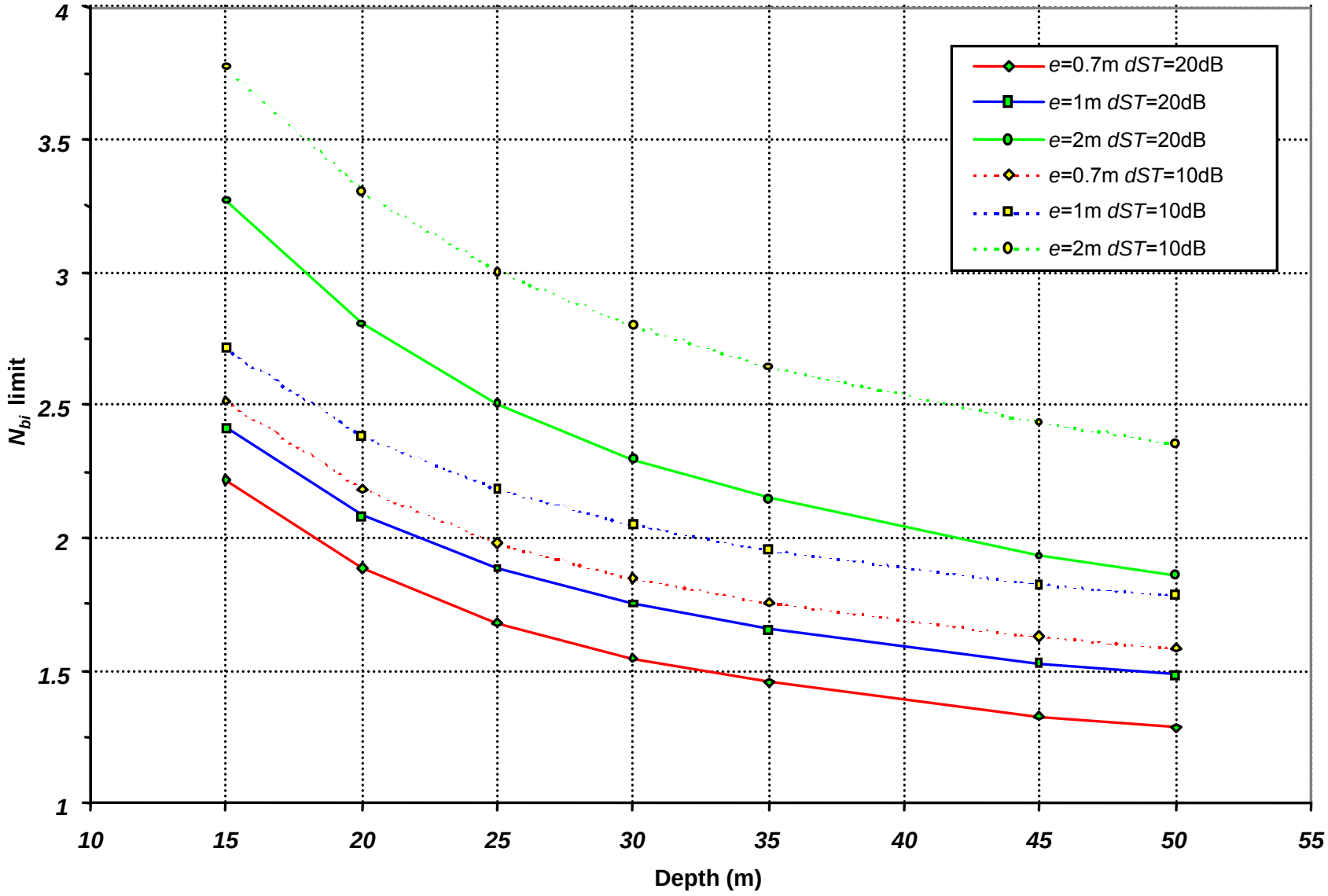
4
3.5
3
2.5
2
1.5
1
N_{bi} limit
10
15
20
25
30
35
40
45
50
55
Depth (m)
e=0.7m dST=20dB
e=1m dST=20dB
e=2m dST=20dB
e=0.7m dST=10dB
e=1m dST=10dB
e=2m dST=10dB

Fig. 6

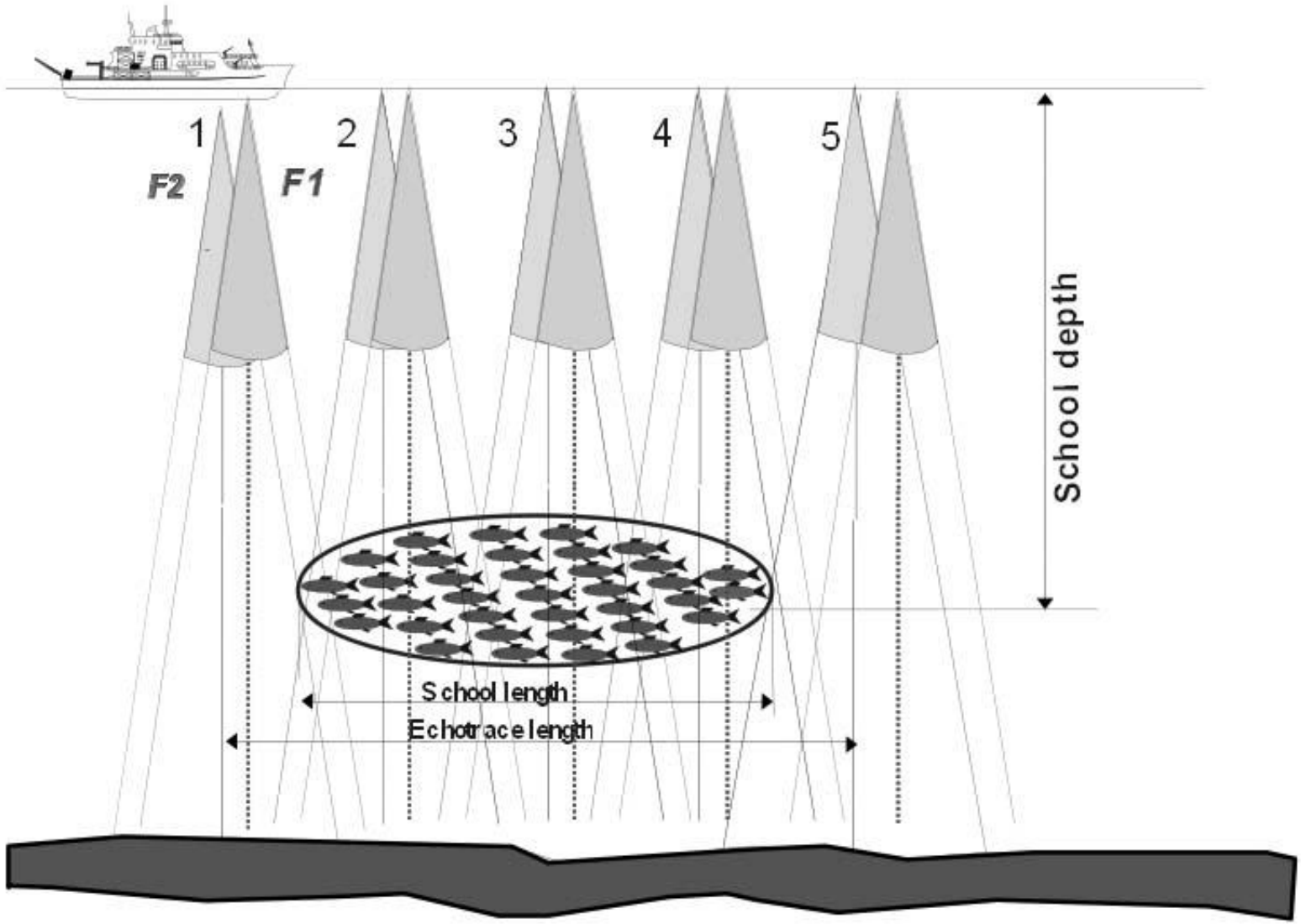

Fig. 7

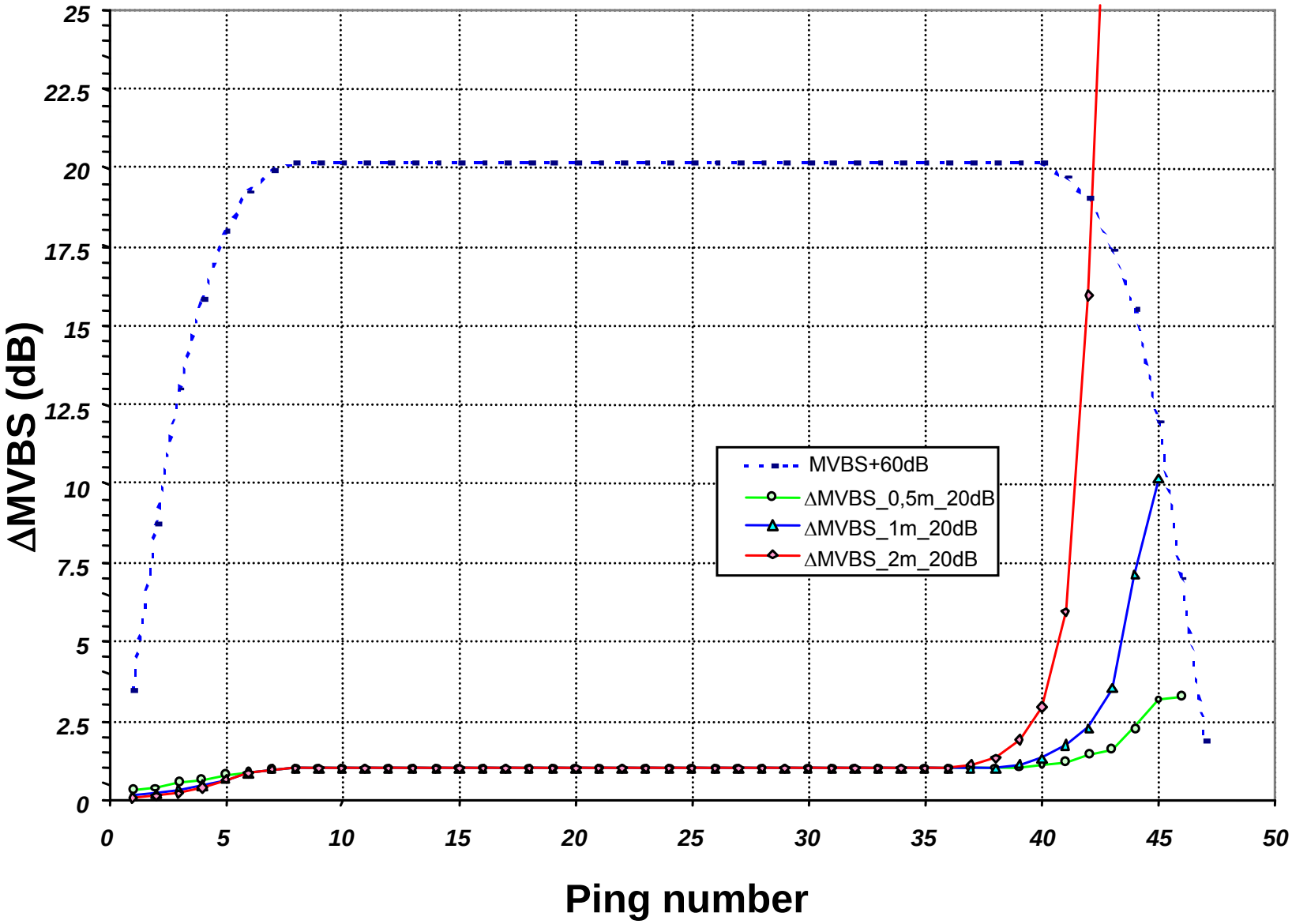
ΔMVBS (dB)
25
22.5
20
17.5
15
12.5
10
7.5
5
2.5
0
0
5
10
15
20
25
30
35
40
45
50
Ping number
MVBS+60dB
ΔMVBS_0,5m_20dB
ΔMVBS_1m_20dB
ΔMVBS_2m_20dB

Fig. 8

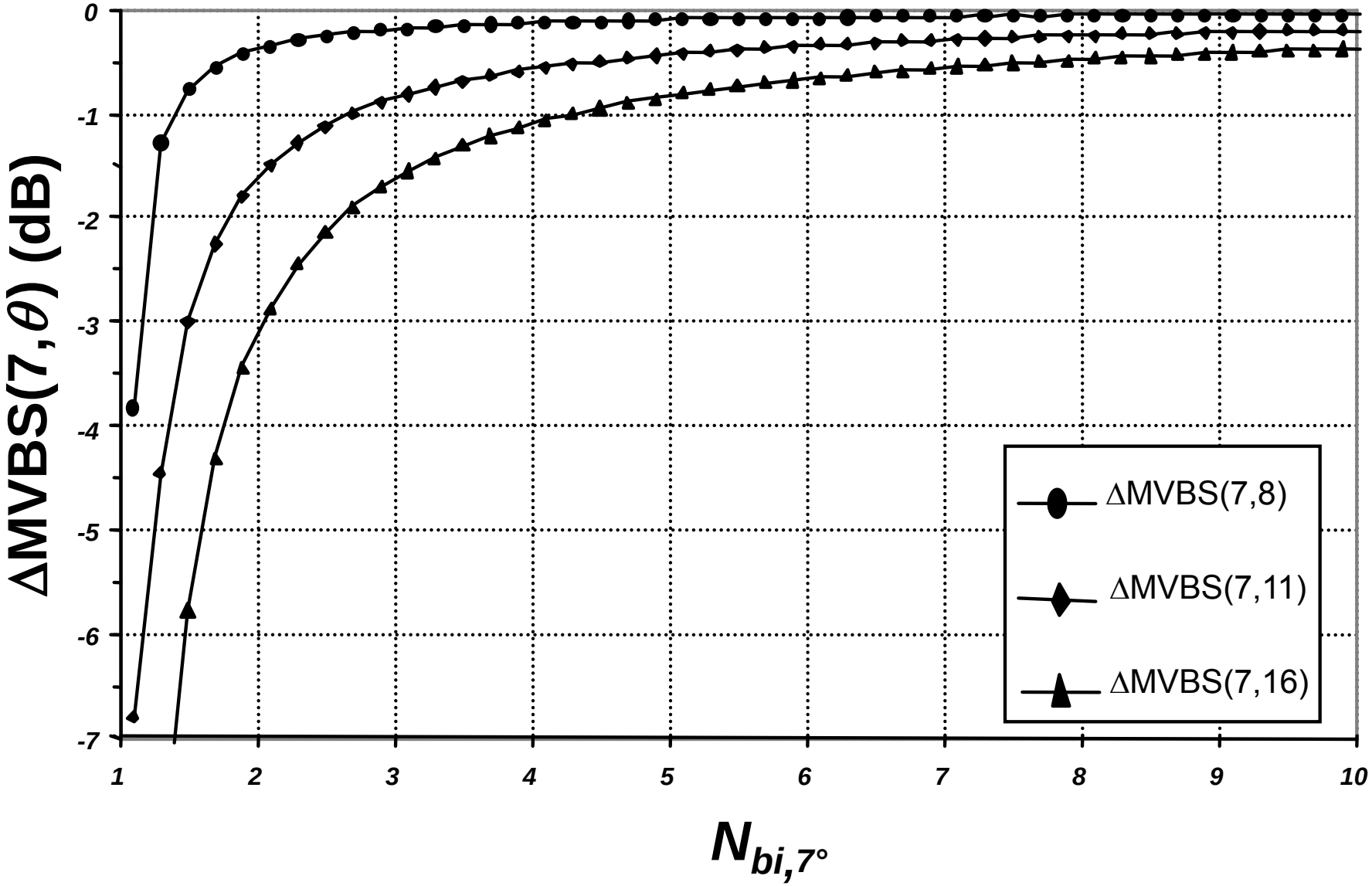
0
-1
-2
-3
-4
-5
-6
-7
ΔMVBS(7,θ) (dB)
1
2
3
4
5
6
7
8
9
10
N bi,7°
ΔMVBS(7,8)
ΔMVBS(7,11)
ΔMVBS(7,16)

Fig. 9.